Supplementary materials

S1. Medium composition All operations described above were carried out in an anaerobic glove box (containing 4% H_2 and 96% N_2, with O_2 concentration below 0.01%). The liquid and solid inorganic salt media share the same basic composition: XAD-7 resin-adsorbed pyrene (~0.05 g/L), 1.7 g/L $NaNO_3$, 0.6 g/L NH_4Cl, 0.61 g/L K_2HPO_4, 0.7 g/L KH_2PO_4, 0.1 g/L $FeCl_2$, 0.1 g/L $CaCl_2$, 0.2 g/L $MgCl_2$, 0.4 g/L $NaHCO_3$, 1 mL/L trace element stock solution, and 1 mL/L vitamin stock solution (Zhang et al., 2021b; Zhang et al., 2021c). During medium preparation, thorough deoxygenation was required, including extended nitrogen sparging and overnight equilibration in an anaerobic glove box. Inoculation was performed only after the addition of 0.1% resazurin redox indicator showed complete decolorization, indicating an anaerobic state (Zhang et al., 2021a).

S2. SEM observation (sample preparation and imaging) Samples for scanning electron microscopy (SEM) were prepared from bacterial cultures harvested at the late logarithmic growth phase. The cultures were firstly centrifuged at 3000 rpm for 10 minutes, and the supernatant was discarded. The cell pellets were resuspended in 2.5% glutaraldehyde and fixed for at least 4 hours. After fixation, the cells were centrifuged again, washed with 1× PBS three times to thoroughly remove residual fixative, and finally resuspended in 1× PBS. Subsequently, a graded ethanol dehydration series was performed using 30%, 50%, 70%, 80%, and 90% ethanol, with each step involving a 10-minute incubation followed by centrifugation and removal of the supernatant (Lee et al., 2020). The cells were then dehydrated three times with

100% ethanol for 30 minutes each. Ethanol was further replaced by tert-butanol through three successive incubations (30 minutes each). The mixed cell–tert-butanol suspension was then dropped onto a slide and vacuum-dried in a freeze-dryer before being viewed with an JSM-7401F field emission scanning electron microscope (Japan).

S3. Gene Ontology analysis procedure To investigate differences and associations in the Gene Ontology (GO) among different strains, GO annotation data were first normalized using $\log_2$ transformation, and a heatmap was generated to visualize functional similarity patterns. Then spearman correlation coefficients were calculated between strains. Principal Coordinates Analysis (PCoA) based on Bray–Curtis distance was conducted to visualize the distributional differences of the strains in terms of their GO functional profiles. To identify key GO terms driving functional differentiation among strains, a random forest classification model was applied. PCoA grouping was used as the response variable, and the top 10 GO categories based on PC1 with the highest explanatory importance were selected. A bar plot was generated to display the importance scores of these selected GO terms.

S4. Carbon-nitrogen metabolism and biofilm-forming genes drive species divergence Analysis of the GO profiles of the nine strains revealed that, among the 42 GO categories, the copy number variation in Cellular Component and Molecular Function terms was minimal, whereas most differences were within Biological Process categories (Fig. S1a). A PCoA of GO-based functional profiles demonstrated clustering patterns that closely mirror the 16S rRNA based phylogeny, indicating that,

despite a high proportion of accessory genes, functional evolution remains tightly linked to vertical inheritance. On the main explanatory axis (PCo1, 70.6% of variance), six of the strains group together, while the larger genome strains KBM-1, PAH1, and W2 are separated only along the secondary axis (PCo2, 16.8% of variance) (Fig. S1b). The top ten GO terms contributing to PCo1 (Fig. S1c) shows that the most discriminating functions involve carbon and nitrogen metabolism and biofilm formation. Enrichment of carbon and nitrogen metabolic processes suggests that these strains can modulate their metabolic strategies to suit varying nutrient conditions, for example, using pollutants as carbon sources under nitrate reducing conditions (Xu et al., 2015; Yang et al., 2024). The amplification of biofilm-related genes likely supports surface colonization and microbial interactions, which are essential for niche establishment and long-term survival under complex environmental stresses (Wei et al., 2023), as they are commonly found to secrete biosurfactants and form biofilms, helping them to survive in a variety of habitats, especially under harsh conditions (Pourfadakari et al., 2019; Naloka et al., 2024).

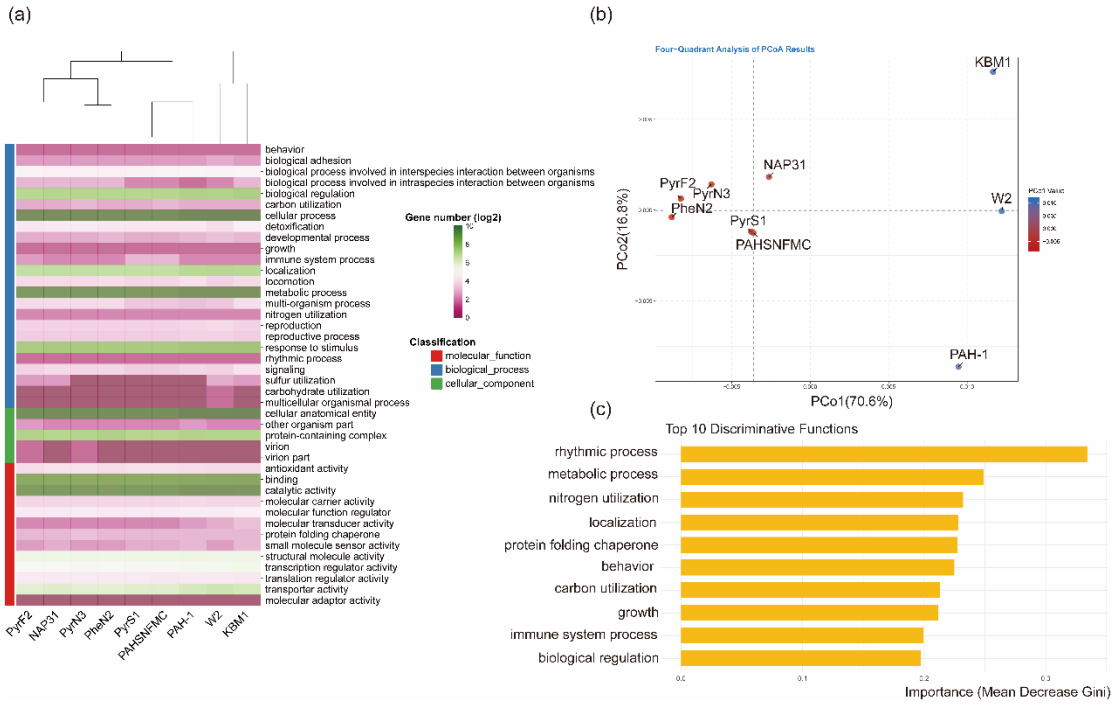

Fig. S1. GO analysis of the nine strains. (a) Heatmap of gene copy numbers (log2) for each GO category across the nine strains. Warmer (more orange) colors indicate higher copy numbers. The x-axis represents the strains; the y-axis groups GO terms into three main categories, color-coded as dark blue for Biological Process, green for Cellular Component, and light blue for Molecular Function. (b) PCoA clustering of the nine strains based on their GO profiles, divided into four quadrants. The first principal coordinate (PCo1) explains 70.6% of the variance, and the second (PCo2) explains 16.8%. (c) The top 10 GO terms most strongly associated with the PCo1 axis.

References

Lee Y C, Hsieh C Y, Chen M L, Wang C Y, Lin C S, Tsai Y H (2020). HighPressure Inactivation of Histamine-Forming Bacteria Morganella Morganii and Photobacterium Phosphoreum. Journal of Food Protection, 83(4): 621-627

Naloka K, Kuntaveesuk A, Muangchinda C, Chavanich S, Viyakarn V, Chen B, Pinyakong O (2024). Pseudomonas and Pseudarthrobacter Are the Key Players in Synergistic Phenanthrene Biodegradation at Low Temperatures. Scientific Reports, 14(1)

Pourfadakari S, Ahmadi M, Jaafarzadeh N, Takdastan A, Neisi A, Ghafari S, Jorfi S (2019). Remediation of PAHs Contaminated Soil Using a Sequence of Soil Washing with Biosurfactant Produced by Pseudomonas Aeruginosa Strain PF2 and Electrokinetic Oxidation of Desorbed Solution, Effect of Electrode Modification with Fe3O4 Nanoparticles. Journal of Hazardous Materials, 379

Wei J, Huang X, Wang H J, Wang F P, Liu X Y, Yan Y, Qu Y H (2023). Insight into biofilm formation of wastewater treatment processes: Nitrogen removal performance and biological mechanisms. Science of the Total Environment, 903

Xu M Y, Zhang Q, Xia C Y, Zhong Y M, Sun G P, Guo J, Yuan T, Zhou J H, He Z L (2015). Elevated nitrate enriches microbial functional genes for potential bioremediation of complexly contaminated sediments. Isme Journal, 9(2): 532-532

Yang L, Lu H Q, Wang Y C, Liu Y C, Tu L X, Meng H Y, Ren Y X, Lan J (2024). Nitrogen Removal Characteristics and Cr(VI) Tolerance Mechanisms of Heterotrophic Nitrifying Bacterium Pseudomonas Putida Strain LX1. Journal of Water Process Engineering, 64

Zhang Z T, Guo H J, Sun J, Gong X Q, Wang C Y, Wang H (2021a). Exploration of the biotransformation processes in the biodegradation of phenanthrene by a facultative anaerobe, strain PheF2, with Fe(III) or O2 as an electron acceptor. Science of the

Total Environment, 750

Zhang Z T, Sun J, Guo H J, Gong X Q, Wang C Y, Wang H (2021b). Investigation of anaerobic biodegradation of phenanthrene by a sulfate-dependent strain PheS2. Journal of Hazardous Materials, 409

Zhang Z T, Sun J, Guo H J, Wang C Y, Fang T T, Rogers M J, He J Z, Wang H (2021c). Anaerobic biodegradation of phenanthrene by a newly isolated nitratedependent strain PheN1 and exploration of the biotransformation processes by metabolite and genome analyses. Environmental Microbiology, 23(2): 908-923